Nuclear Saturation and Two-Body Forces. II. Tensor Forces

K. A. BRUECKNER
Department of Physics, Indiana University, Bloomington, Indiana
(Received June 7, 1954)

The method developed in a previous paper for the treatment of the problem of nuclear saturation has been extended to the case of tensor forces. The general result obtained expresses the many-body potential energy as a function of the triplet and singlet eigen phase shifts for scattering. One consequence is that the tensor force, which averages to zero if Born approximation is used to evaluate the scattering, now gives a very sizable contribution to the potential energy. Phase shifts have been determined for a specific potential model derived from pseudoscalar meson theory, and are shown to give scattering up to 90 Mev which is in good agreement with total cross section and in approximate agreement with angular distributions. Use of these results to evaluate the total energy (neglecting Coulomb effects) in heavy nuclei shows that for a typical case ($A=300$) saturation occurs at a radius $1.15\times10^{-13}A^{\frac{1}{3}}$ with a binding energy of 10 Mev per particle. If surface effects are neglected, however, the density at saturation increases by a factor of 1.74 with an increase in mean binding energy to 39 Mev. The potential energy per particle has also been determined as a function of its momentum. In the finite nucleus ($A=300$) the potential depth varies from -82 Mev for a particle of zero momentum to -32 Mev for a particle at the top of the Fermi momentum distribution. Arguments are presented which suggest that this effect is to a large extent independent of the model used.

I. INTRODUCTION

In a previous paper[1] (to be referred to as I) the relation of nuclear saturation to two-body forces was discussed making use of an approximation method which allowed an exact treatment of the coherent particle motion in the nucleus. This method is in essence an "optical model" approximation in that the potential felt by a particle is expressed as an average of the forward scattering amplitudes over the nuclear momentum states. In such an approximation, coherent modes of motion appear which are particle-like but which are not simply related (except in an average sense) to the motion of a "bare" nucleon. Thus the "independent particle" given by the model does not refer to "independent nucleon" motion but rather refers to a type of collective aspect of the nuclear state. The detailed relationship of the approximation methods of I and of this paper to other models and methods will form the content of a paper to be published separately.

In I it was found that if tensor forces (which average to zero in first approximation) and surface effects were neglected, two-body potentials derived from meson theory[2] and in agreement with low-energy scattering parameters were sufficient in themselves to give saturation with about the correct values of density and binding energy, i.e., $R=1.15\times10^{-13}A^{\frac{1}{3}}$ cm, $E=-12$ Mev. It is the purpose of this paper to consider the effects of tensor forces and also to compare the scattering amplitudes used with the nucleon-nucleon scattering over the range of energies which are important in the saturation problem. We shall also discuss some of the simplest surface effects which arise from the modification (by the finite surface) of the nuclear states. We shall not, however, in this paper discuss the Coulomb effects or the tendency of the tensor force to distort the nucleus.

In Sec. II we shall summarize briefly the formulas which we shall need in our consideration of the saturation problem with tensor forces and discuss the computational techniques used in determining the phase shifts for scattering; in Sec. III we shall compare with experiment the scattering predicted by the potentials we have used; in Sec. IV the effects of finite nuclear size will be discussed; in Sec. V the saturation problem will be evaluated; and finally in Sec. VI some concluding remarks will be made.

II. FORMALISM

In I it was shown that in order to determine the effective "potential" in the saturation problem, it was sufficient to evaluate the sum

$$\langle V\rangle=\tfrac{1}{2}\sum[(\mathbf{k}_i,\mathbf{k}_j|t'_{\rm ord}|\mathbf{k}_i,\mathbf{k}_j)-(\mathbf{k}_j,\mathbf{k}_i|t'_{\rm exch}|\mathbf{k}_i,\mathbf{k}_j)], \quad (1)$$

where the t''s are the scattering amplitudes in the momentum states $\mathbf{k}_i$, $\mathbf{k}_j$ evaluated at the kinetic energies in the nuclear medium. $t'_{\rm ord}$ and $t'_{\rm exch}$ are, respectively, the ordinary and exchange matrix elements of the scattering amplitudes. This result is further expressible in terms of the scattering amplitudes in the forward direction in the substates of spin and isotopic spin, which we denote by $a_{s\lambda}$ where s indicates the spin state and λ the isotopic spin state. As a function of these, the potential energy is

$$V=-\frac{4A}{\pi m}\int_0^{k_F}P(k)dk[a_{ss}+3a_{ts}+3a_{st}+9a_{tt}], \quad (2)$$

with $P(k)$ the probability (unnormalized) of finding the relative momentum k in the nuclear ground state. It is this integral which we wish to express in terms of the

[1] Brueckner, Levinson, and Mahmoud, Phys. Rev. **95**, 217 (1954).
[2] K. A. Brueckner and K. M. Watson, Phys. Rev. **92**, 1023 (1953).

phase shifts for scattering with the tensor force effects included. It is clear that in this treatment we do not consider the possible effects on the energy arising from spin polarization and distortion of the nucleus from a spherical shape; these are specifically surface effects and small compared with both the volume energy and with the simple surface effect which we discuss in Sec. V.

We further remark here that any contribution to the scattering which is due to the tensor force and which can be legitimately treated in Born approximation gives no contribution to the integral of Eq. (2). This result is the consequence of the averaging to zero of the tensor force operator upon spin averaging and is the analog in our method of the absence of a tensor force contribution in an uncorrelated medium.

It is next convenient to summarize formulas for tensor scattering which express the phase shifts in terms of the eigen phase shifts of the scattering matrix. In this we make use of results which are implicit in the work of Blatt and Biedenharn.[3] An explicit derivation of these formulas is given in Appendix A. For the singlet scattering and for the uncoupled triplet states (with $L=J$), this introduces no change from the usual results. For the coupled triplet states with $L=J\pm1$, however, application of the results of Blatt and Biedenharn leads to useful relations between the usual phase shifts (functions of LJm) and the eigen phase shifts. In the notation of Blatt and Biedenharn, we have (see Appendix A):

$$\begin{aligned}
\eta_{J-1}{}^{J,\pm1}&=(\tan\epsilon+\cot\epsilon)^{-1}\{\cot\epsilon\eta_\alpha+\tan\epsilon\eta_\beta\\
&\qquad-[J/(J+1)]^{\frac{1}{2}}(\eta_\alpha-\eta_\beta)\},\\
\eta_{J+1}{}^{J,\pm1}&=(\tan\epsilon+\cot\epsilon)^{-1}\{\tan\epsilon\eta_\alpha+\cot\epsilon\eta_\beta\\
&\qquad+[J/(J+1)]^{-\frac{1}{2}}(\eta_\alpha-\eta_\beta)\},\\
\eta_{J-1}{}^{J,0}&=(\tan\epsilon+\cot\epsilon)^{-1}\{\cot\epsilon\eta_\alpha+\tan\epsilon\eta_\beta\\
&\qquad+[J/(J+1)]^{-\frac{1}{2}}(\eta_\alpha-\eta_\beta)\},\\
\eta_{J+1}{}^{J,0}&=(\tan\epsilon+\cot\epsilon)^{-1}\{\tan\epsilon\eta_\alpha+\cot\epsilon\eta_\beta\\
&\qquad-[J/(J+1)]^{\frac{1}{2}}(\eta_\alpha-\eta_\beta)\},
\end{aligned}\tag{3}$$

where

$$\eta_L{}^{Jm}=\sin\delta_L{}^{Jm}e^{i\delta_L{}^{Jm}},\quad \eta_\alpha=e^{i\delta_\alpha}\sin\delta_\alpha,\quad \text{etc.}\tag{4}$$

The eigen phase shift δ_α is the $L=J-1$ dominant phase shift; at low energy as the mixing parameter ϵ goes to zero, the scattering in a given J state is dominated by the $L=J-1$ state.

Application of the formulas of Eq. (3) leads to simple expressions for the forward scattering amplitudes averaged over spins. We denote the coupled phase shifts by $\eta^{\pi}{}_{J\sigma s}(\sigma=\alpha,\beta)$ where $\pi=-(-1)^J$ is the parity, and the uncoupled states by $\mu^{\pi}{}_{JLs}$. Application of the usual scattering formulas[4] then gives for the four substates of spin and isotopic spin:

$$\begin{aligned}
ka_{ss}&=\sum_{J\text{ odd}}\mu^{-}{}_{JJ0}(2J+1),\\
ka_{st}&=\sum_{J\text{ even}}\mu^{+}{}_{JJ0}(2J+1),\\
3ka_{ts}&=\sum_{J\text{ odd}}(2J+1)(\eta^{+}{}_{J\alpha1}+\eta^{+}{}_{J\beta1})\\
&\qquad+\sum_{J\text{ even}\geqq2}(2J+1)\mu^{+}{}_{JJ1},\\
3ka_{tt}&=\sum_{J\text{ even}}(2J+1)(\eta^{-}{}_{J\alpha1}+\eta^{-}{}_{J\beta1}+\mu^{+}{}_{JJ1})\\
&\qquad+\sum_{J\text{ odd}}(2J+1)\mu^{-}{}_{JJ1}.
\end{aligned}\tag{5}$$

For the triplet odd states (a_{tt}) the scattering is rather weak and may be treated in Born approximation; for this reason the tensor contribution averages out in the saturation calculation for this state. Thus we may write for a_{tt} the simpler expression

$$ka_{tt}=\sum_{L\text{ odd}}(2L+1)\mu^{-}{}_{L}(c),\tag{6}$$

where $\mu^{-}{}_{L}(c)$ is determined by the central odd-state potential alone.

We note that the results of Eq. (5) depend on the eigen phase shifts alone, the parameter ϵ having dropped out on performing the spin sum. We also remark at this point that we take proper account of the standing wave boundary condition[5] which is correct in the saturation problem by replacing the complex $e^{i\delta}\sin\delta$ by $\tan\delta$. It is here that the convenience of expressing the scattering in terms of the eigen phase shifts is apparent since it is only in terms of the eigen states that a stationary description of the problem is possible.

The phase shifts for the coupled $J=1$ even parity state were determined by numerical integration of the coupled equations; as a check, an iteration in the integral equations was made. Two independent solutions were constructed by so choosing the amplitudes and slopes at the core as to satisfy the orthogonality condition.[6] From these two solutions, the eigen states and mixing parameter were determined following the methods of Appendix A. For the remaining states, the potential for the uncoupled D waves is quite strong so that this phase shift was determined by numerical integration. The other D phase shifts were determined by Born approximation, as were the quite small P-wave phase shifts, both coupled and uncoupled.

III. SCATTERING RESULTS

The intimate connection between the saturation calculation and the scattering phase shifts which is characteristic of the methods used in I and in this paper makes a parallel discussion of both desirable. We shall

[3] J. Blatt and L. C. Biedenharn, Phys. Rev. **86**, 399 (1952).
[4] See, for example, J. Ashkin and Ta-You Wu, Phys. Rev. **73**, 973 (1948).
[5] B. A. Lippmann and J. Schwinger, Phys. Rev. **79**, 469 (1950).
[6] W. Rarita and J. Schwinger, Phys. Rev. **59**, 436 (1941).

therefore in this section describe the scattering[7] which is predicted by the phase shifts we are to use in the discussion of saturation. These have been determined for the meson theory potentials we have specifically considered.[2] First, we shall qualitatively describe the p-p scattering as given by our results and the comparison with experiment.[8,9] The calculated cross section together with the experimental results are shown in Fig. 1. The potentials we use are characterized by quite short range in the singlet state and by a nonmonotonic quite strong tensor force together with a weak central force in the odd state. The combined effect of these is the following: at 32 Mev, the small D-wave scattering (0.80° D phase shift) is almost completely masked by the quite appreciable tensor scattering (peaked at 90°) which combines with the central scattering (peaked at 0°) to give an almost isotropic scattering. The magnitude of the scattering is slightly larger than the experimental results; the tendency of the S-wave repulsion to diminish the S-wave scattering is only slightly felt at this energy. At 90 Mev, the central scattering now shows very pronounced S-D interference which, however, is still masked completely by the tensor scattering which gives a quite appreciable fraction of the scattering. The resulting cross section (nuclear scattering only) is still quite isotropic; the cross section is rather small with the rapidly dropping S phase showing the core effect. The magnitude of the scattering is perhaps

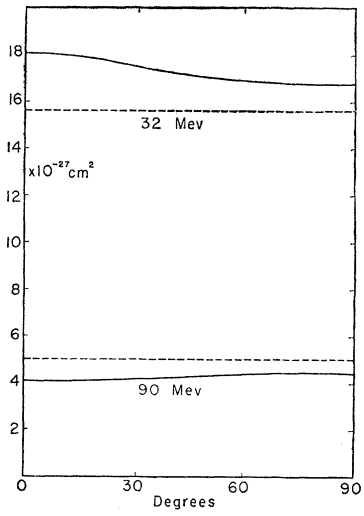

FIG. 1. Differential cross sections in the center-of-mass system for p-p scattering at 32[8] and 90[9] Mev, neglecting Coulomb effect. The experimental results are well fitted by pure S-wave nuclear scattering; the magnitudes of the nuclear scattering alone which agree with the experimental results are shown by the dashed curves.

[7] In this section we have drawn extensively on the ideas and results of R. Christian and E. Hart, Phys. Rev. **77**, 441 (1950); R. Christian and H. P. Noyes, Phys. Rev. **79**, 85 (1950).

[8] W. K. H. Panofsky and F. L. Fillmore, Phys. Rev. **79**, 57 (1950); Cork, Johnson, and Richman, Phys. Rev. **79**, 71 (1950).

[9] R. W. Birge, Phys. Rev. **80**, 490 (1951); R. W. Birge, Phys. Rev. **83**, 274 (1951).

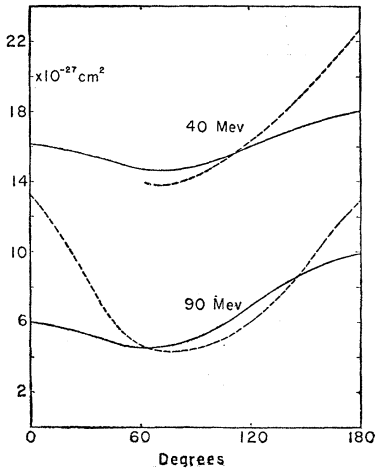

FIG. 2. Differential cross sections in the center-of-mass system for n-p scattering at 40[11] and 90[12] Mev. The solid curves are calculated; the dashed curves represent an approximate fit to the experimental results.

slightly too small although not outside of the experimental errors, and is actually in good agreement with a recently reported value[10] of 4.6 millibarns for the differential cross section at 90 degrees. These results show certainly a good agreement with the high-energy p-p scattering and, of course, agree with the low-energy scattering data which were used in determining the parameters of the potential.

The situation is not quite so satisfactory in the n-p scattering. The potentials in this case are more complicated than in the p-p case with twice as many states (because of the effects of the exclusion principle) and the even-odd state interference makes the analysis less simple. Qualitatively, the potentials which did not act on the p-p system are characterized by the dominant tensor force in the triplet even state and the strong repulsion in the singlet odd state. The even-state tensor force gives most of the scattering of the partial waves of high angular momenta since it is of considerably larger range than the very short-tailed central triplet even force. The cross section drops quite rapidly in magnitude as the repulsive cores affect the S-wave scattering quite appreciably even at 40 Mev.

The quantitative results of the scattering at 40 and 90 Mev are given in Fig. 2. It is apparent that although the cross sections in magnitude agree very well with the experimental results,[11,12] they are in error to some extent in having somewhat too much exchange scattering and too little scattering of high partial waves; i.e., the odd-state potentials are somewhat too strongly repulsive, and the even-state potentials are not long-tailed enough. It is possible that these difficulties might

[10] V. E. Kruse and J. M. Teem, Phys. Rev. **95**, 662 (A) (1954).

[11] Hadley, Kelley, Leith, Segrè, Wiegand, and York, Phys. Rev. **75**, 351 (1949); R. Hildebrand and C. E. Leith, Phys. Rev. **76**, 587 (1949).

[12] O. Chamberlain and J. W. Easley, Phys. Rev. **94**, 208 (1954). This paper gives a list of references to earlier work.

be eliminated by alteration of the potentials we have used. In view of the semiquantitative agreement, however, and of the great arbitrariness which enters in much alteration of the interactions, we have not at present made further investigation of the origin of the detailed discrepancies. It might be pointed out, however, that the difficulty appears to originate in the too short-tailed character of the triplet even-state potentials which can be altered without upsetting the good agreement of the predicted p-p scattering with experiment.

In concluding this section, we remark that the agreement with experiment of the scattering predicted by the phase shifts we have calculated is quantitatively quite good, particularly in the p-p scattering. We therefore feel that the use of these scattering amplitudes in the saturation discussions of Sec. V will not introduce appreciable errors. This is particularly true since most of the contribution to the potential energy comes from rather low relative momenta (corresponding to energies in scattering of less than 40 Mev) where the agreement with experiment is particularly good.

IV. SURFACE EFFECTS

Before proceeding to a discussion of the saturation problem, we shall develop some results which we use in the next section. Specifically, we shall discuss a surface effect which in this model appears to be of particular importance, i.e., the effect of the finite nuclear volume on the distribution of momentum states. This effect appears very directly in the kinetic energy which is increased when the nuclear particles are localized in a finite volume. A further effect arises from the alteration of the distribution of states of relative momentum for two colliding particles which has a pronounced effect on the potential energy.

To account for this effect in an approximate (and very simple) way, we make use of a result of Wheeler and Hill[13] who show approximately that the number of states per momentum interval (assuming spherical symmetry) is given by

$$N(k)d\mathbf{k}=\left(\frac{v}{2\pi^2}-\frac{s}{16k\pi}\right)\frac{d\mathbf{k}}{4\pi}, \tag{7}$$

where v is the total volume and S is the surface area. In this expression a small term linear in the nuclear dimensions has been dropped. For a spherical nucleus, this can be written

$$N(k)d\mathbf{k}=v\frac{d\mathbf{k}}{(2\pi)^3}[1-3\pi/4kR], \tag{8}$$

where R is the nuclear radius. We note that the number of states goes to zero at

$$k=3\pi/4R\equiv k_0, \tag{9}$$

which is reasonable since

$$\lambda_0=2\pi/k_0=8R/3, \tag{10}$$

is approximately the longest wavelength which can have nodes in the nuclear volume ($\frac{1}{2}$ wave falling in the nucleus). (The factor $8R/3$ appearing instead of $4R$ represents a crude correction for the surface curvature.) Thus, we write

$$N(k)d\mathbf{k}=\frac{vd\mathbf{k}}{(2\pi)^3}\left(1-\frac{k_0}{k}\right). \tag{11}$$

The total number of particles (with 4 per momentum state) is

$$A=\frac{4v}{(2\pi)^3}\frac{4\pi}{3}k_F^3(1-\tfrac{3}{2}k_0/k_F), \tag{12}$$

defining K_F as a function of A, the density, and of k_0 (or of R). Further, we have for the mean kinetic energy

$$T=\frac{4}{A}\int\frac{k^2}{2M}N(k)d\mathbf{k}=\frac{vk_F^5}{5AM\pi^2}\left(1-\frac{5}{4}\frac{k_0}{k_F}\right). \tag{13}$$

These results can be expressed conveniently in terms of the limiting case of $A\to\infty$ for constant density. In this case we introduce the dimensionless density parameter η by the relation

$$v=(4/3)\pi R^3=(4/3)\pi r_0^3\eta^3A, \tag{14}$$

where r_0 is the mean spacing between nuclear particles ($r_0=1.40\times10^{-13}A^{\frac{1}{3}}$ cm) and η is accordingly of the order of one. In terms of this parameter, the Fermi momentum for an infinite medium is

$$k_\infty=(9\pi/8)^{\frac{1}{3}}(r_0\eta)^{-1}=1.52\mu/\eta. \tag{15}$$

Using Eq. (9) for k_0, we finally find

$$\frac{k_F}{k_\infty}=\left[1-\tfrac{3}{4}(3\pi^2)^{\frac{1}{3}}\frac{k_\infty}{k_F}A^{-\frac{1}{3}}\right]^{-\frac{1}{3}}, \tag{16}$$

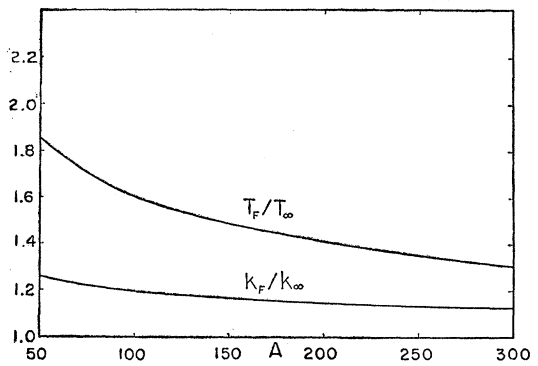

FIG. 3. Effects at constant density of finite nuclear size on the maximum momentum k_F and the average kinetic energy T_F in the degenerate Fermi gas. The ratios of k_F and T_F to k_∞ and T_∞ (k_F and T_F for an infinite medium) are given.

[13] D. L. Hill and J. A. Wheeler, Phys. Rev. **89**, 1102 (1953).

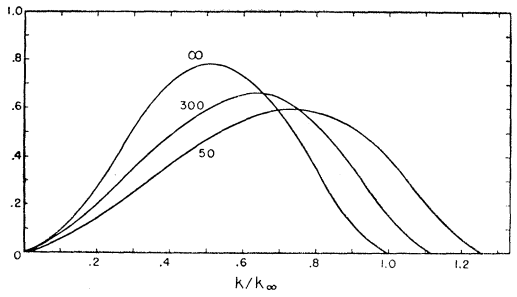

FIG. 4. Probability of the relative momentum k in a degenerate Fermi gas, showing surface effect. The vertical scale is arbitrary; the horizontal scale is in units of k_∞.

and

$$\frac{T_F}{T_\infty}=\left(\frac{k_F}{k_\infty}\right)^5\left[1-\tfrac{5}{8}(3\pi^2)^{\frac{1}{3}}\frac{k_\infty}{k_F}A^{-\frac{1}{3}}\right]^{\frac{1}{3}}. \tag{17}$$

These results for k_F/k_∞ and T_F/T_∞ are given in Fig. 3 as a function of A.

We next need the effect from this change in the momentum distribution on the distribution of relative momenta. In evaluating the potential energy, we encounter an integral of the form

$$\int N(k_1)d\mathbf{k}_1N(k_2)d\mathbf{k}_2f(\tfrac{1}{2}\mathbf{k}_1-\tfrac{1}{2}\mathbf{k}_2)\Big/\int N(k_1)d\mathbf{k}_1. \tag{18}$$

Transforming to relative and total momentum coordinates and introducing the results of Eq. (11), we find for this integral

$$32\pi\int_0^{k_F}dkf(k)P(k), \tag{19}$$

where $P(k)$ is the probability (unnormalized) of finding a relative momentum k, and is equal to (with $x=k/k_F$)

$$\begin{aligned}P(k)=k^2\left(1-\frac{3}{2}\frac{k_0}{k_F}\right)^{-1}&\left[1-\tfrac{3}{2}x+\tfrac{1}{2}x^3-3\frac{k_0}{k_F}(1-x-\tfrac{2}{3}x^2)\right.\\&\left.+3\left(\frac{k_0}{k_F}\right)^2(1-\tfrac{3}{2}x)\right],\quad x\leqslant\tfrac{1}{2};\\=k^2\left(1-\frac{3}{2}\frac{k_0}{k_F}\right)^{-1}&\left[1-\tfrac{3}{2}x+\tfrac{1}{2}x^3\right.\\&-3\frac{k_0}{k_F}\left(-x+\tfrac{2}{3}x^2+\frac{1}{3x}\right)\\&\left.+3\left(\frac{k_0}{k_F}\right)^2\frac{1}{2x}(1-x)^2\right],\quad x\geqslant\tfrac{1}{2}.\end{aligned} \tag{20}$$

This distribution is given in Fig. 4 for several values of A. The shift to higher values of relative momentum with decreasing radii is evident.

V. SATURATION

A. Average Energies

We now proceed to relate the results of the preceding sections to the saturation problem. The phase shifts which we need are simplified by the averaging out of all tensor force contributions which need be considered only in Born approximation. For this reason, the tensor force affects only the coupled ^3S-^3D and the remaining D phase shifts. The contributing states are shown in Figs. 5, 6, and 7. In evaluating the integrals over relative momenta which give the potential energy, the passage of the large phase shift δ_α through 90° at a relative momentum of about 0.64 μc gives rise to a singularity in the integrand (as $\tan\delta_\alpha$ passes through the singularity at $\delta_\alpha=\pi/2$). This does not give any difficulty, however, since the integral about this point has the character of a principal value and the integration through the pole gives a finite result, the contribution from the vicinity of the pole actually giving only a small contribution to the result. It might be remarked that the occurrence of this pole is a consequence of the presence of a bound state for the triple even state.

The energy is finally determined as a function of the number of particles and of the density by use of Eqs. (2), (5), (6), (20), and the values for the phase shifts. These results are given in Fig. 8. They show the remarkably large effect of the surface, not only in the kinetic energy but also to about the same extent in the volume energy. It is perhaps not possible to take these results entirely seriously since the treatment in which surface effects are so important is probably less reliable than the treatment of a volume effect alone. Nevertheless, it is difficult to believe that these effects do not exist to a very considerable extent in nuclear structure in any model. They represent qualitatively very reasonable modifications in the kinetic energy (due to restriction in volume) and in volume energy (due to shift to population to higher momenta and hence to less strongly interacting states).

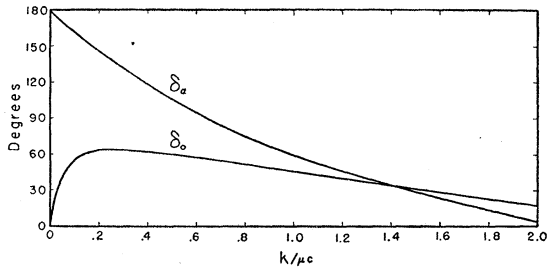

FIG. 5. Singlet $S(\delta_0)$ and S-dominant $J=1$ even-parity (δ_α) phase shifts. The abscissa is in units of $\mu c=140$ Mev/c.

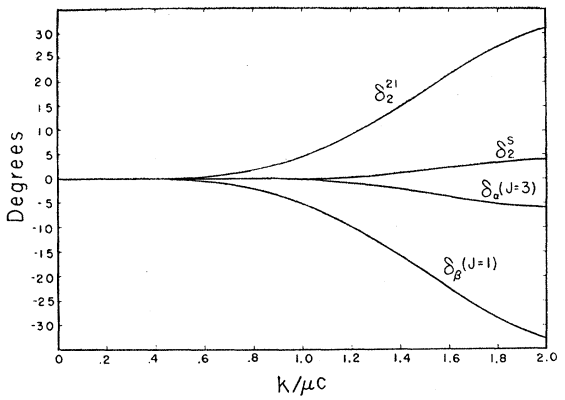

FIG. 6. D phase shifts for coupled [$\delta_\beta(J=1)$ and $\delta_\alpha(J=3)$] and uncoupled (δ_2^{21}) triplet states and for singlet state (δ_2^{s}).

B. Energies as a Function of Particle Momentum*

We can also obtain more detailed information about the characteristics of particle motion in the nuclear medium. A particularly interesting result is the dependence of the interaction energy on the momentum of the particle being considered. We get this result by integrating in the potential energy only over the momenta of one of the colliding particles. This gives an expression:

$$V(k)=\frac{2}{\pi M}\int_0^{\frac{1}{2}(k+k_F)} f(k')P(k',k)dk', \qquad (21)$$

where $f(k')$ is the same statistically weighted sum of amplitudes that appears in the integral of Eq. (2), and $P(k,k')$ is the probability of finding the relative momentum k'; using Eq. (11) for the density of momentum states, this function is

$$P(k',k)=\mu_{\max}-\mu_{\min}-(k_0/k)[(k^2+4k'^2+4kk'\mu_{\max})^{\frac{1}{2}} - (k^2+4k'^2+4kk'\mu_{\min})^{\frac{1}{2}}], \qquad (22)$$

where

$$\mu_{\max}=\text{lesser of}\left\{1,\frac{k_F^2-k^2-4k'^2}{4kk'}\right\},$$
$$\mu_{\min}=\text{greater of}\left\{-1,\frac{k_0^2-k^2-4k'^2}{4kk'}\right\}. \qquad (23)$$

* *Note added in proof.*—Because of an oversight by the author, a factor of two was omitted in Eq. (21) for $V(k)$ which should read

$$V(k)=\frac{4}{\pi M}\int_0^{\frac{1}{2}(k+k_F)} f(k')P(k',k)dk'. \qquad (21')$$

This factor is necessary since in calculating the average potential energy, it is necessary to take account of the origin of the potential energy in two-body forces. Thus the correct relation between $\bar{V}$ and $V(k)$ is

$$\bar{V}=\frac{1}{2}\int_0^{k_F} V(k)k^2dk \Big/ \int_0^{k_F} k^2dk, \qquad (21'')$$

the factor $\frac{1}{2}$ arising from the fact that the integrations of Eqs. (21′) and (21″) are equivalent to summing over all particles twice. $\bar{V}$ defined by Eqs. (21′) and (21″) is identical with that given by Eq. (2).

As a result of this correction, all values for $V(k)$ in Fig. 9 and Fig. 10 should be multiplied by two. Consequently the anomaly of unbound surface particles discussed in the conclusion does not arise.

The result of the integration of Eq. (21) for the potential energy as a function of k is given in Figs. 9 and 10 for the cases of 300 nucleons and of an infinite number. The rapid change of the depth with energy reflects the much stronger scattering at low values of relative momentum.

C. Discussion

The tensor force makes its presence strongly felt in the saturation, even when nuclear distortion is not considered, through its marked enhancement of the low energy triplet even state scattering. This effect, which is absent in the conventional saturation calculation without correlation, increases the average potential energy per particle by roughly 40 percent and at the same time increases the rate of increase of potential energy with increasing density. The net effect relative to the calculation neglecting tensor effects is not only to increase considerably the average binding in an infinite medium (from 12 Mev to 39 Mev) but also to decrease the equilibrium radius from $1.15\times10^{-13}A^{\frac{1}{3}}$ cm to $0.85\times10^{-13}A^{\frac{1}{3}}$ cm. These effects for an infinite medium are, however, to some extent compensated in a finite medium by the effects of the surface on both the kinetic and potential energies so that in a heavy nucleus ($A=300$) the binding energies and equilibrium radius again take on reasonable values.

VI. CONCLUSIONS

We have derived formulas which relate the many-body potential energy to the characteristics of two-body scattering, for the general case of central and noncentral forces. We have also evaluated approximately the effects of the nuclear surface when the number of interacting nucleons is finite. Combining these results with a set of phase shifts derived from an explicit potential model (which gives scattering in semiquantitative agreement with experiment), we obtain the energy per particle in nuclear matter as a function of the density, the number

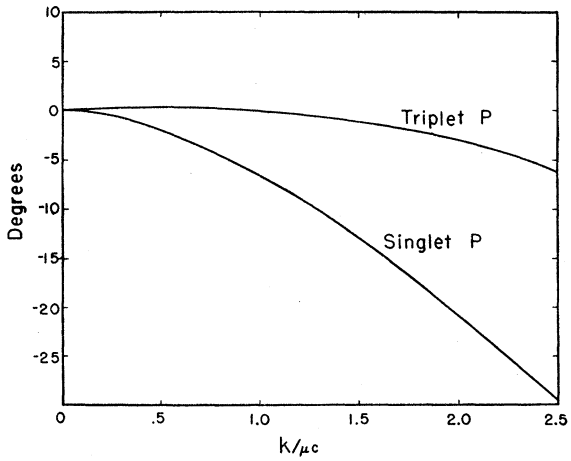

FIG. 7. P phase shifts neglecting tensor force. The core radius in the triplet states has been taken to be $0.4\hbar/\mu c$.

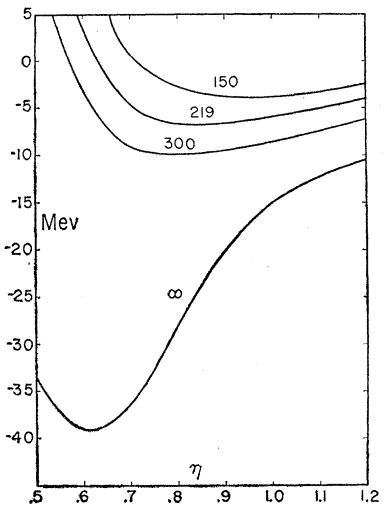

FIG. 8. Average energy per particle as a function of density and of total number of particles. The density parameter η is defined in Eq. (14).

of nucleons, and the momentum of the particle. These results show that in the absence of surface effects, the binding energy per particle is 39 Mev at an equilibrium radius of $R=0.85\times10^{-13}A^{\frac{1}{3}}$ cm, and thus that saturation in the usual sense does not occur at normal density. These results differ markedly from the results of I, where central forces alone were considered, in that the strong low energy scattering arising from the tensor force considerably increases the interaction energy for low momentum encounters. This effect is, of course, absent in a method which treats the scattering in Born approximation and which further assumes uncorrelated nucleon positions.

If, however, a finite nucleus is considered (as, for example, with 300 nucleons) the surface effects increase the kinetic energy and decrease the potential energy with the net result that a more reasonable value of binding energy of 10 Mev per particle results at an equilibrium radius of $1.15\times10^{-13}A^{\frac{1}{3}}$ cm. These modifications are the consequence of the alteration in the density of momentum states (compared with a Fermi gas), and are analogous to a surface energy with origin in both kinetic and potential effects. Such effects are a natural consequence of the specific model used but would also appear in a qualitatively similar way in any model which attempts to deduce the potential of an "independent particle" model from the two-body interactions.

Another striking effect is the strong dependence of the potential felt by a particle on the particle momentum, reflecting the decrease in the scattering amplitudes as the relative momentum in collision increases. This behavior almost certainly is present, in a qualitative form at least, in any nuclear model treating particle motion to a first approximation as independent. The size of the effect can be seen in Fig. 10 which shows the decrease in potential energy from -82 Mev at zero momentum to -32 Mev at the top of the Fermi distribution. A curious anomaly appears here also in that the relatively weak potential felt by the rapidly moving particles of maximum kinetic energy results in a positive total energy; i.e., these particles are unbound. The precise meaning of this result depends on a thorough understanding of the nature of the nuclear surface, and more particularly, of the relation to the nucleons of the independent particle modes of the coherent motion. It is not clear, for example, that the requirement of binding for the physical nucleons is not more closely related to the average binding of the coherent modes than to the binding of the mode of highest momentum.

In conclusion we would like to comment that further extension of the methods of the previous paper (I) and of this paper cannot be made until the nature of the nuclear surface and of the "particle" coupling to the surface is understood. The strikingly large effect of the surface considered somewhat crudely in this paper shows the importance of a quantitative understanding of the surface phenomena. These topics form a subject outside of the scope of this paper; it is expected that work along these lines will be published separately in the near future.

The author is indebted to Dr. C. A. Levinson and Dr. H. Mahmoud for helpful discussions of some of the topics of this paper, and to Professor John A. Wheeler for a very stimulating discussion of the implications of these results. The author would also like to acknowledge the computational aid of Dr. John Chappelear.

APPENDIX A. TENSOR SCATTERING AND EIGEN PHASE SHIFTS

We consider the scattering in a state with total angular momentum J, parity $\pi=-(-1)^J$, and with two coupled orbital angular momentum states with $L=J\pm1$. We introduce the eigenstates of the scattering

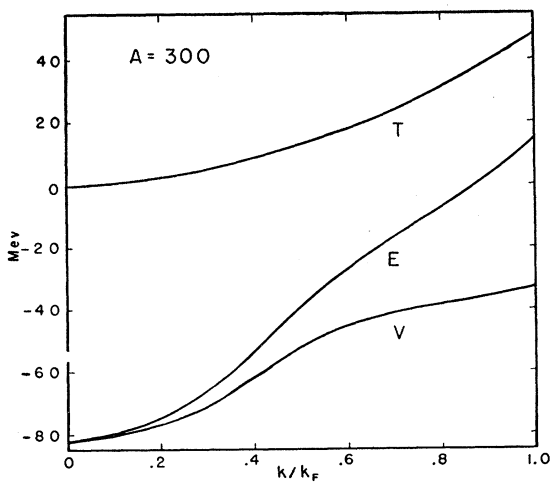

FIG. 9. Potential, kinetic, and total energy per particle in an infinite medium as function of momentum. The abscissa is measured in units of the Fermi momentum. The evaluation has been carried out at the equilibrium density indicated in Fig. 8.

matrix which are characterized by the fact that in scattering, such states experience the same phase shift in the two coupled states with $L=J\pm1$. These states we call $g_{J\alpha}{}^m$ and $g_{J\beta}{}^m$; they have, respectively, the asymptotic forms

$$g_{J\alpha}\sim\frac{\mathcal{Y}_{J,J-1}{}^m-\tan\epsilon\mathcal{Y}_{J,J+1}{}^m}{1+\tan^2\epsilon}\frac{\sin[kr-\frac{1}{2}\pi(J-1)+\delta_\alpha]}{kr},$$
$$g_{J\beta}\sim\frac{\mathcal{Y}_{J,J-1}{}^m+\cot\epsilon\mathcal{Y}_{J,J+1}{}^m}{1+\cot^2\epsilon}\frac{\sin[kr-\frac{1}{2}\pi(J-1)+\delta_\beta]}{kr}, \tag{A1}$$

where ϵ is the real parameter which determines the asymptotic ratio of $L=J-1$ and $L=J+1$ states in the eigenstate and δ_α, δ_β are the eigen phase shifts. We use these equations to define generalized spherical harmonics

$$I_{J\alpha}{}^m(\epsilon)=(\mathcal{Y}_{J,J-1}{}^m-\tan\epsilon\mathcal{Y}_{J,J+1}{}^m)(1+\tan^2\epsilon)^{-1},$$
$$I_{J\beta}{}^m(\epsilon)=(\mathcal{Y}_{J,J-1}{}^m+\cot\epsilon\mathcal{Y}_{J,J+1}{}^m)(1+\cot^2\epsilon)^{-1}, \tag{A2}$$

or collectively, introducing the transformation coefficients $B(JLm|J\sigma m)$,

$$I_{J\sigma}{}^m=\sum_L B(JLm|J\sigma m)\mathcal{Y}_{JL}{}^m,\quad \sigma=\alpha,\beta, \tag{A3}$$

and their inverses

$$\mathcal{Y}_{JL}{}^m=\sum_{\sigma=\alpha,\beta}B(J\sigma m|JLm)I_{J\sigma}{}^m. \tag{A4}$$

With this notation it is now simple to get expressions for the phase shifts in terms of the eigen phase shifts and the transformation coefficients $B(JLm/J\sigma m)$. First we write the total wave function in the asymptotic region

$$\psi_J{}^m=\sum_{\sigma=\alpha,\beta}A_\sigma I_{J\sigma}{}^m\sin[kr-\tfrac{1}{2}\pi(J-1)+\delta_\sigma]/kr. \tag{A5}$$

The incoming wave is

$$\psi_0{}^m=\sum C_L Y_L{}^0\chi_1{}^m\sin(kr-\tfrac{1}{2}\pi L)/kr$$
$$=\sum C_L C(JLm|SL0m)B(J\sigma m|JLm)I_{J\sigma}{}^m \times\sin(kr-\tfrac{1}{2}\pi L)/kr, \tag{A6}$$

where the $C(SLm_Lm_S|JLm)$ are the usual Clebsch-Gordan coefficients. Using this result and choosing the coefficients A_σ in such a way as to have only outgoing spherical waves, we find

$$\psi_J{}^m=\psi_{0J}{}^m+\psi_J{}^m-\psi_{0J}{}^m$$
$$=\psi_{0J}{}^m+\frac{e^{ikr}}{kr}\sum C_L C(JLm|SL0m) \times B(J\sigma m|JLm)(-i)^L I_{J\sigma}{}^m(e^{2i\delta\sigma}-1)/2i. \tag{A7}$$

To get the conventional expression in terms of the usual phase shifts, we re-express the $I_{J\sigma}{}^m$ in terms of the spherical harmonics to find

$$\psi^m=\psi_0{}^m+\frac{e^{ikr}}{kr}\sum C_{L'} \times C(JL'm|SL'0m)B(J\sigma m|JL'm)(-i)^{L'} \times B(JLm|J\sigma m)C(SLm-m_s'm_s'|JLm) \times\frac{e^{2i\delta\sigma}-1}{2i}Y_L{}^{m-m_s'}\chi_1{}^{m_s'}. \tag{A8}$$

In terms of the usual complex phase shifts $\delta_L{}^{Jm_s}$, the wave function has the form

$$\psi^m=\psi_0{}^m+\frac{e^{ikr}}{kr}\sum C_L i^L\frac{[\exp(2i\delta_L{}^{Jm_s})-1]}{2i} \times C(SLm_s-m_s'm_s'|JLm_s) \times C(JLm|SL0m)Y_L{}^{m_s-m_s'}\chi_1{}^{m_s'}. \tag{A9}$$

Comparison of Eqs. (A8) and (A9) gives:

$$\frac{\exp(2i\delta_L{}^{Jm_s})-1}{2i}=\sum_{L'\sigma}\frac{C(JL'm|SL'0m)}{C(JLm|SL0m)} \times B(J\sigma m|JL'm)B(JLm|J\sigma m) \times\left(\frac{2L'+1}{2L+1}\right)^{\frac{1}{2}}\frac{e^{2i\delta\sigma}-1}{2i}. \tag{A10}$$

Using the transformation coefficients $B(J\sigma m|JLm)$ and their inverses, we finally get for $m=\pm1$,

$$\eta_{J-1}{}^{J,\pm1}=(\tan\epsilon+\cot\epsilon)^{-1}[\cot\epsilon\eta_\alpha+\tan\epsilon\eta_\beta -(J/J+1)^{\frac{1}{2}}(\eta_\alpha-\eta_\beta)],$$
$$\eta_{J+1}{}^{J,\pm1}=(\tan\epsilon+\cot\epsilon)^{-1}[\tan\epsilon\eta_\alpha+\cot\epsilon\eta_\beta +(J/J+1)^{-\frac{1}{2}}(\eta_\alpha-\eta_\beta)]. \tag{A11}$$

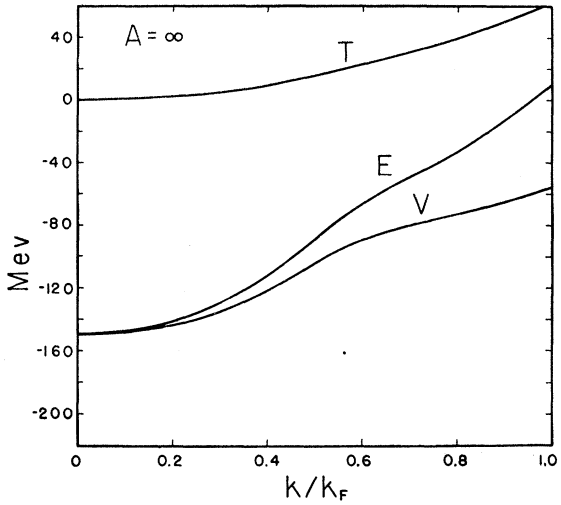

FIG. 10. Potential, kinetic, and total energy per particle for a "nucleus" made up of 300 nucleons (with $Z=N$) as a function of momentum. The evaluation is at equilibrium density.

And for $m=0$

$$\eta_{J-1}{}^{J,0}=(\tan\epsilon+\cot\epsilon)^{-1}[\cot\eta_\alpha+\tan\eta_\beta+(J/J+1)^{-\frac{1}{2}}(\eta_\alpha-\eta_\beta)],$$
$$\eta_{J+1}{}^{J,0}=(\tan\epsilon+\cot\epsilon)^{-1}[\tan\eta_\alpha+\cot\eta_\beta-(J/J+1)^{\frac{1}{2}}(\eta_\alpha-\eta_\beta)], \quad \text{(A12)}$$

where

$$\eta_L{}^{Jm}=\exp(i\delta_L{}^{Jm})\sin\delta_L{}^{Jm}, \text{ etc.}$$

Thus the phase shifts for a given J are expressed in terms of the real parameters ϵ, δ_α, δ_β.

To make use of these formulas, it is further necessary to show how the parameter and the eigen phase shifts may in practice be determined from the solutions which are obtained in the numerical solutions of the coupled tensor equations. We suppose that two independent solutions satisfying the boundary conditions have been determined, as for example by so choosing the amplitudes and slopes at the core as to satisfy the orthogonality condition.[6] These solutions are asymptotically of the form (we consider the $J=1$ even parity state)

$$\psi_i{}^m=\sin(kr+\delta_i)\mathcal{Y}_{101}{}^m+\beta_i\sin(kr-\pi+\sigma_i)\mathcal{Y}_{121}{}^m, \quad \text{(A13)}$$

where δ_i and σ_i are the (in general unequal) phase shifts for the S and D waves and β_i is a parameter determining the relative asymptotic amplitude of S and D waves. From these two solutions we construct the linear combinations

$$\psi_\rho{}^m=\psi_1{}^m+\rho\psi_2{}^m. \quad \text{(A14)}$$

If we now impose the condition that the phase shift in the S and D waves be equal, thus determining the eigen phases, we find a condition on ρ and further an expression for $\tan\delta_\rho$,

$$\frac{\sin\delta_1+\rho\sin\delta_2}{\cos\delta_1+\rho\cos\delta_2}=\frac{\beta_1\sin\sigma_1+\rho\beta_2\sin\sigma_2}{\beta_1\cos\sigma_1+\rho\beta_2\cos\sigma_2}=\tan\delta_\rho. \quad \text{(A15)}$$

This gives a quadratic equation for ρ; the two roots determine the two eigen phase shifts. Thus we can write for the solution $\psi_\alpha{}^m$:

$$\psi_\alpha{}^m=A_\alpha[\sin(kr+\delta_\alpha)\mathcal{Y}_{101}{}^m+\tan\epsilon\sin(kr+\delta_\alpha-\pi)\mathcal{Y}_{121}{}^m], \quad \text{(A16)}$$

where $\tan\epsilon$ from comparison with Eq. (A1) is, using Eq. (A15),

$$\tan\epsilon=\frac{\beta_1\sin\sigma_1+\rho_\alpha\beta_2\sin\sigma_2}{\sin\delta_1+\rho_\alpha\sin\delta_2}. \quad \text{(A17)}$$

This completes the construction from the two original solutions of the necessary parameters.

PHYSICAL REVIEW VOLUME 96, NUMBER 2 OCTOBER 15, 1954

Space-Time Representation in Wave Mechanics: Illustration of the Method

MALCOLM K. BRACHMAN
Texas Instruments Incorporated, Dallas, Texas
(November 12, 1953)

The basic equations of a new space-time representation are derived in a heuristic fashion, and a simple application is presented to illustrate the point of view.

A NEW space-time representation has been developed by Hellund and the present author.[1] This paper provides a heuristic derivation of the Schrödinger equation in the new representation and illustrates its solution by considering the square-well potential.

THE SCHRÖDINGER EQUATION

We consider a one-dimensional system with a Hamiltonian $H(-i\hbar\partial/\partial x, x)$ in the Schrödinger representation. The Hamiltonian is assumed to have the form

$$H=-\frac{\hbar^2}{2m}\frac{\partial^2}{\partial x^2}+V(x)=T+V. \quad (1)$$

The wave function $\Psi(x,t)$ satisfies the Schrödinger equation

$$H\Psi=i\hbar(\partial\Psi/\partial t). \quad (2)$$

Our task is to find the form of this equation in the new representation.

The one-dimensional space is split into cells by the points of division $x=L_\sigma$, $\sigma=0,\pm1,\pm2,\cdots$, with $L_0=0$. The σth cell is bounded by the abscissas L_σ and $L_{\sigma-1}$, and its length is $l_\sigma=L_\sigma-L_{\sigma-1}$. In the σth cell there is an orthonormal set of functions, $\varphi_{j\sigma}(x)$, which is defined only within the cell. These functions may be conveniently chosen to be of exponential form, and may be written

$$\varphi_{j\sigma}(x)=\frac{h(\sigma)}{\sqrt{l_\sigma}}e^{ik_{j\sigma}x},\ j=0,\pm1,\pm2,\cdots. \quad (3)$$

[1] E. J. Hellund and M. K. Brachman, Phys. Rev. 92, 822 (1953).